Dynamic Modeling Based Optimal Design of a Crash Helmet

A. Chawla[1], S. Kadam[2] and S. P. Singh[3]

[1]Indian Institute of Technology, New Delhi; achawla@mech.iitd.ernet.in
[2]formerly at Indian Institute Of Technology; New Delhi; c/o achawla@mech.iitd.ernet.in
[3]Indian Institute Of Technology; New Delhi; singhsp@mech.iitd.ernet.in

ABSTRACT

This work aims at optimizing a helmet. First a discrete dynamic model of a helmet has been proposed for modeling the free fall of the helmet from a height of 2m. The model was solved using Runge Kutta method. The time history of head acceleration has been extracted from this solution and 'Time bound peak acceleration criteria' of head injury has been computed After preparing the model it was validated using available experimental and FEM results. The model was then used for optimization. The objective of optimization is to minimize 'time bound peak acceleration' which is taken as an injury criterion representing the effectiveness of the helmet. The optimization is constrained to a maximum total mass and total thickness of the helmet. The optimization has been carried out using conventional method as well as genetic algorithms. Subsequently the sensitivity of the objective function with respect to different design parameters was studied.

Keywords: Dynamic modeling, Injury criteria, Drop test, Stiffness, Damping, Optimization.

1. INTRODUCTION

In day today life we observe many cases of two wheeler accidents. Helmets a re a primary safety device used on motor cycles. A well-designed crash helmet has proved to be a very good protection device against head injuries in road accidents. The use of helmets reduces the number of fatal injuries as well as the severity of the injuries from 45 to 80% [13],[16]. Most of the work done in the field of helmets is based on experimental techniques [18],[11] or on FEM [1]. Hopes and Chinn [11] have examined the existing helmets by experimentation. They have suggested various changes to improve the effectiveness of the helmets. They have discussed different head injury criterions and their appropriateness. Goldsmith Werner [7] has also done detail study of head injury and its relation to different head injury criteria. Gilchrist and Mills [2],[7],[12] have studied different types of helmets and their performance with different materials and geometry. They have also worked on mathematical modeling of effectiveness of helmets. In the present work, basic guidelines for the dynamic modeling are derived from [12]. However instead of using concrete experimental data for getting the material properties, we seek to make a completely mathematical model and the material properties are also expressed mathematically as a function of design parameters. This makes the model suitable for use for optimization.

Different head injury tolerances or criteria have been used in literature to define its biomechanical safe limit. Some of the important criterion are Head Injury criteria (HIC), Head Performance Criteria (HPC), Gadd Severity Index (SI) and the Peak Acceleration Criteria [7]. The Time Bound peak acceleration (TBPA) criteria specifies the peak acceleration over a specified time limit; e.g. peak acceleration of head should not exceed 200g for 2msec or 150g for 4 msec [7]. This is simple and easy to implement and is used in the present work.

The present work aims at optimizing the motorcycle crash helmets. The application and construction of helmets is studied and appropriate materials are selected for different parts of the helmet. Thereafter a dynamic model of the helmet is prepared. This model predicts the dynamic behavior of the helmet under impact for given values of design variables. A bio-mechanical limit for head injury based on acceleration time history of the head is adopted. The model is validated using available experimental and FEM results. It is then optimized by minimizing the head injury criteria. The optimization is subjected to constraints on maximum weight and total thickness of the helmet. Thus the present work seeks to obtain optimal values of design parameters of helmet.

2. METHODOLOGY

In order to design the helmet, the steps followed for problem solving are as follows. First a discrete dynamic model of

the helmet was prepared. The model has three degrees of freedom. In the model, we consider the mass of shell, foam layer and head form. The stiffness and damping for each layer has been modeled accordingly. The model was solved using Runge-Kutta method and the acceleration, displacement and velocity time history of helmet during impact were obtained. The model was then validated using available experimental data. After validating and approving the model, the variation in the behavior of the system was studied with respect to different design parameters. The helmet design was then optimized for minimum TBPA subject to the constraints on mass and thickness of the helmet. In this study polystyrene is taken as material for inner foam layer whereas glass reinforced plastic is taken as material of shell.
The following assumptions are made in this study while preparing the model:

- The surface which impacts the helmet is rigid.
- The headform is rigid.
- Forces developed in the helmet are local
- Area of contact of the helmet with the impacting surface is circular
- The comfort Foam absorbs negligible amount of energy. So its mass, stiffness and damping are not considered in the modeling.
- Global bending of the helmet is negligible.

3. DYNAMIC MODELING

The helmet consists of the outer shell, foam layer and a comfort layer as shown in Fig. 1. During the impact siulation, a headofrm representing the head is taken to be inside the helmet as shown. A three degree of freedom discrete dynamic model of the helmet is prepared. The model constitutes of three masses representing the head form, outer shell and inner foam layer (Fig. 3). The downward direction is considered as positive through out this paper.

3.1 Mathematical Model

Applying Newton's law we get the following equations of motion:

$$m_h\ddot{x}_h + k_f\left(x_h - x_f\right) + c_f\left(\dot{x}_h - \dot{x}_f\right) = 0$$

$$m_f\ddot{x}_f + k_s\left(x_f - x_s\right) - k_f\left(x_h - x_f\right) + c_s\left(\dot{x}_f - \dot{x}_s\right) - c_f\left(\dot{x}_h - \dot{x}_f\right) = 0$$

$$m_s\ddot{x}_c - k_s\left(x_f - x_s\right) - c_s\left(\dot{x}_f - \dot{x}_s\right) + k_c x_s + c_c\dot{x}_s = 0$$

Where, m_f, m_h and m_s stand for mass of foam, head and shell respectively, x_h, x_f, x_s stand for displacements of the foam, head and shell and k_c, k_f and k_s stand for stiffnesses of contact, foam and shell respectively. These equations have been solved using Runge-Kutta method. The stiffness and damping needed in these equations are non-linear and their values change with deformation of the component.
When the helmet falls vertically on the ground the contact area is taken to be circular. From the geometry of impact area, as shown in Fig. 2, the radius of the contact circle can be calculated as:
$A = \pi a^2 = \pi\left(R^2 - (R-x)^2\right) = 2\pi Rx + x^2$ where A = Contact Area = Shaded Area for $x << R$, a is the radius of the area of contact, R is the helmet radius and x is the deformation.

3.1.1 Foam Stiffness Modeling

The second layer of helmet is made up of polystyrene foam. In modeling foam stiffness the stress strain curve of polystyrene (under impact) is used. The curve has been taken from [9] and is shown in Fig. 4. It can be observed from the curve that, the loading part of the stress strain curve is independent of the strain rate. For all strain rates the same curve called master curve is traced, but the return path changes as the strain rate changes. This curve has three major regions – the elastic region, plastic region and return path. All these regions follow different rule of stress strain relationship and the stiffness is modeled accordingly in these regions.
The first part of the curve is the elastic region in which stress - strain satisfies the Hook's law i.e. stress is directly proportional to strain ($\sigma = E\,\varepsilon$) and the stiffness of the foam can be shown to be

$k_f = \dfrac{2 * \pi * R * \left(x_h - x_f\right) * E_f}{t_f}$, where E_f is the Young's Modulus of the foam and t_f is the foam thinckness.

The second region is the plastic region of the curve. In this region stress strain relations are no more linear. The stress strain relation is taken as [9] $\sigma = \left(\sigma_o + \dfrac{p_o\varepsilon}{1-\varepsilon-D}\right)$, where σ is the stress in the foam, σ_o is a constant, p_o is the initial gas pressure (atmospheric) in the foam, ε is the strain in the inner foam layer and D is the Relative Density of Foam ($D = \rho_0/\rho_f$), ρ_0 and ρ_f being the density of solid foam and density of foam respectively.

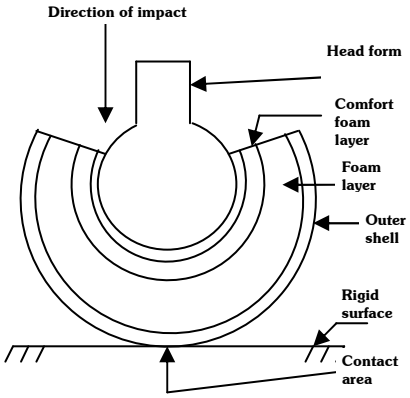

Fig. 1. The helmet with the headform.

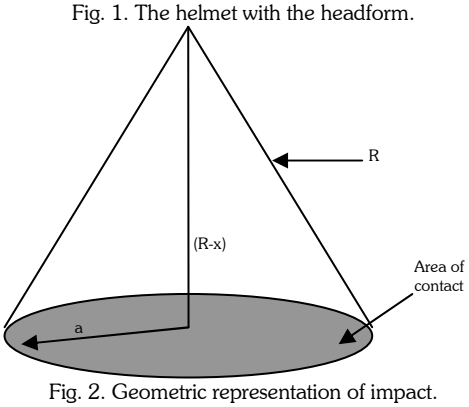

Fig. 2. Geometric representation of impact.

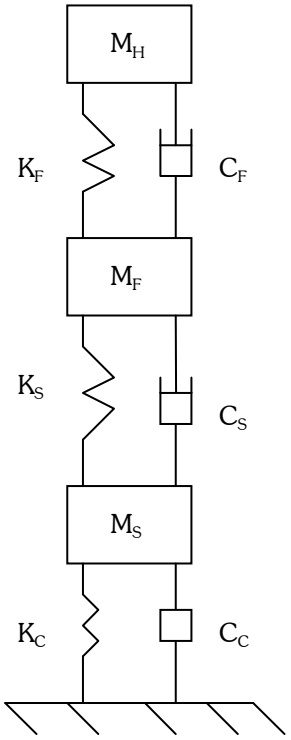

Fig. 3. Dynamic Model Of Helmet.

The stiffness in this case comes out to be

$$k_f = \left(\sigma_0 + \frac{p_o\left(x_h - x_f\right)}{1-\left(x_h - x_f\right) - D * t_f}\right) * \left(2 * \pi * R\right)$$

The return path from the peak point is also nonlinear. While it is approximately linear for low strain rates, the non-linearity increases as the strain rate increases. Here the return path is approximated as a straight line parallel to the elastic region line. So this line will have slope same as that of elastic region line but it will not pass through the origin. It is assumed that reloading follows the same path. The stress strain relation for this region can be expressed as $\sigma = E_f \varepsilon + const$, where E_f is the Young's modulus for the foam and the value of the constant can be found using the peak point (return point) co-ordinates. The stiffness in this region can be found out using the following equation:

$$k_f = \left(E_f * \varepsilon + const\right) * 2 * \pi * r_f$$

As has been seen earlier the material properties of foam depend upon relative density and properties of the base material i.e. solid polymer. Empirical relation between relative density and other properties of foam (e.g Young's modulus , density, strength) are given by [9] $E_f = E_0 * D^{1.5}$, where $E_0 = 3 * 10^9 N/m^2$, $Y_f = Ys * D^{1.5}$, where $Y_s = 6 * 10^7 N/m^2$ and $\rho_0 = 1200 kg/m^3$. Our program calculates values of material properties of foam using above relations and then uses these values to evaluate the stiffness of the foam.

3.1.2 Shell Stiffness Modeling

The shell material is assumed to be orthotropic composite material. It will have different values of Young's modulus in perpendicular directions. As the impact is in transverse direction, Young's Modulus in transverse direction is used. As has been seen, the properties of the composite depend on fiber as well as matrix material and volume fraction of the two [4]. The relation between transverse Young's modulus (E_t) of fiber (subscript f) and matrix (subscript m) and that of the composite (subscript c) can be expressed as follows [4]:

$E_{ct} = \dfrac{E_{ft} * E_{mt}}{V_f * E_{mt} + V_m * E_{ft}}$, where $V_m = 1 - V_f, E_{mt} = 3.2 * 10^9 N/m^2. E_{ft} = 2 * 10^9 N/m^2$, V_f is the fraction of the fibre.

For the matrix, as it is a homogeneous material, $E_{ml} = E_{mt}$. Compressive strength of the composite is obtained by dividing compressive strength of the matrix by a stress concentration factor, generally taken as 1.5. This stress concentration factor accounts for the stress concentration due to fibers.

$f_{cc} = f_{mc}/1.5$ and $f_{mc} = 158e6\,N/m^2$; where f_{cc} is the compressive strength of the composite and f_{mc} is that of the matrix.

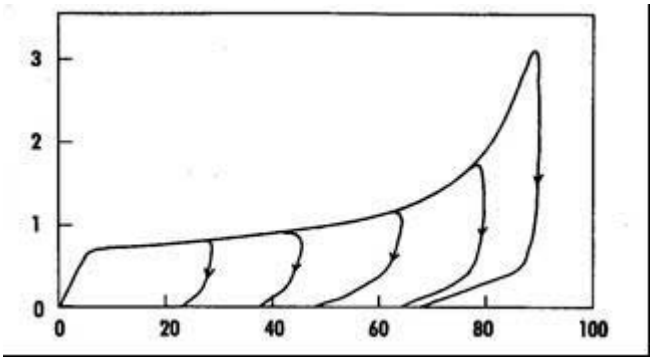

Fig. 4. Stress Strain Relation for polystyrene (X Axis shows the strain (%), Y Axis shows stress(1*10 ^ 10 Pa).

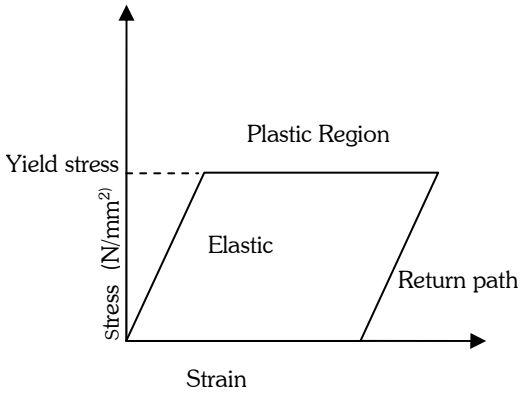

Fig. 5. Stress Strain Relationship for shell material.

Glass reinforced plastic has been used as the material for shell. As the material is plastic in nature, it has been modeled as elasto-plastic. A typical stress-strain variation for a elasto-plastic material is shown in Fig 5. It can be seen from the figure that upto the yield stress, Hook's law is followed but after that the curve is parallel to X- axis. Unloading is parallel to the loading curve. The later loading curve follows the unloading path. Stiffness has been modeled differently for elastic and plastic regions as per the corresponding laws.

In the elastic region the stress-strain satisfies the Hooke's law i.e. stress is directly proportional to strain, $\sigma = E_{cs}\varepsilon$, where Ecs is the compressive Young's Modulus for the shell. Hence, the stiffness in the elastic region is given by

$$k_c = \frac{E_{2s} * \left(x_f - x_s\right) * 2 * \pi * r_s}{t_s}$$

In the plastic region, the stress strain relation is represented by a horizontal line parallel to the x-axis. Here total force is given by Force = yield stress*area, and the stiffness is therefore given by

$k_s = \left(f_{ct}\right) * \left(2 * \pi * r_s\right)$

The return path is a straight line parallel to the elastic region line. So using a similar approach the stiffness becomes,

$k_s = \left(E_{cs} * \varepsilon + const\right) * 2 * \pi * r_f$

3.1.3 Contact Stiffness Modeling

During impact of the helmet, the outer shell as well as foam layer of the helmet bends locally as well as globally. In local bending, the shell bends near the impact region whereas in global bending the whole shell tends to bend about the impact point. This bending poses stiffness at the contact. While modeling the contact stiffness global bending has been neglected. Fig. 6 demonstrates the local and global bending of the shell. After bending, the shell becomes flat as shown in Fig. 7. The shell tries to regain its original shape back and thus acts as a spring. This gives rise to renounce of the helmet. The bending has been modeled as shown in Fig. 8. Here it is assumed that the load at the contact surface is uniformly distributed over the contact area. If 'w' is the deformation at the center in the X-direction, and 'p' is the pressure acting on the shell, then the relation between deformation and pressure is given by [5] $w = \frac{p * R^2}{2 * E_{cs} * t_s}$. Here if total contact force is f_s, pressure 'p' is given by $p = \frac{Force}{Area} = \frac{f_s}{2 * \pi * R * x_s}$.

Modifying the above expression we get, $w = \frac{f_s * R}{4 * \pi * x_s E_{cs} * t_s}$. Thus stiffness is given by

$$k_c = \frac{f_s}{w} = \frac{4 * \pi * x_s * E_{2c} * t_s}{r_c}$$

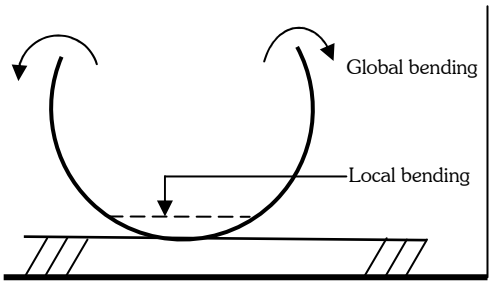

Fig. 6. Global and local bending.

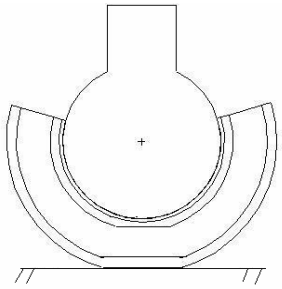

Fig. 7. Helmet after local bending.

3.1.4 Stiffness in Tension

The stiffnesses modeled up till now are stiffnesses due to compression of the material or bending. As soon as the compression becomes zero the head and foam, and the shell and foam lose contact with each other. So there will be no shell stiffness or foam stiffness in tension. Mathematically this can be expressed as :

For $x_h - x_f < 0, k_f = 0$, For $x_f - x_s < 0, k_s = 0$ and for $x_s < 0, k_c = 0$.

3.1.5 Modeling of Damping

Damping is an important element of the helmet model. Primarily, in both foams and shell viscoelastic type of damping is present. In case of plastics or polymers viscous as well as elastic effects are observed. So these are called viscoelastic materials. In these materials when stress is applied, corresponding response is sluggish which leads to time lag between stress and strain. Different models have been developed to represent this behavior of viscoelastic materials [8],[14]. Kelvin-Voigt model has been used in the present work.

As per Hook's law, stress is directly proportional to the instantaneous strain. But this is not applicable to viscoelastic materials as there is phase difference between stress and strain. Kelvin modeled the viscous behavior [8] with a spring and a damper in parallel as shown in Fig. 9. The spring represents force proportional to strain and damping represents force proportionate to strain rate. If a load P is imposed at time t=0, then from equation, the subsequent deflection X(t) can be given by :

$$X(t) = \left(\frac{P}{k}\right) * \left(1 - e^{-t/\tau}\right)$$

τ is called retardation time. It is a ratio of damping to stiffness. In this equation, for actual materials the value of the constant 'retardation time' depends upon molecular structure, strain rate, peak stress level, variation in stresses etc. According to Gilchrist and Mills, in case of helmet impacts, for ensuring realistic hysteresis in the loading and unloading sequence, the retardation time should be 0.25 msec for foam and 0.2 msec for shell [6],[7] i.e. $c_f = 0.25*10^{-3} * k_f$, $c_s = 0.2 *10^{-3} * k_s$, $c_c = 0.2 *10^{-3} * k_c$., where c_f, c_s and c_c are the damping in the foam, shell and contact respectively These relations are used to evaluate the damping incorporated in the dynamic model.

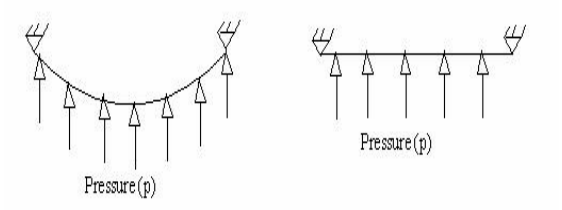

Fig. 8. : Modeling of local bending.

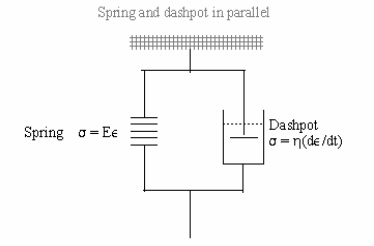

Fig. 9. Kelvin-voigot model.

3.1.6 Mass Modeling

To model helmet mass, a simple geometry of the helmet is assumed. The helmet has been optimized for this particular shape. It is assumed that the helmet is made up of two sections. The upper section is approximated as elliptical in shape. It is half ellipse as shown in Fig. 10a. The lower section is taken as a partial elliptical cylinder as shown in Fig. 10b.

The inner radius of the helmet generally ranges from 90 to 110 mm whereas the total radius of the helmet (outer radius of the outer shell) ranges from 125-140 mm. In the present work the inner radius is taken as base dimension and other dimensions are found out using it. The inner radius is taken to be 100mm.
Let R be the inner radius of the helmet. Then the average radius of the foam layer can be taken as $r_f=R+t_f/2$, that of the shell will be $r_s = R+t_f+t_s/2$ and the radius of the outer shell is $r_c=R+t_f+t_s$.
Next step is to find out volume of the foam and shell. Let a_i, b_i and c_i be the inner dimensions of the ellipsoid. After studying the dimensions of the available helmets, the relation between ellipsoid dimensions and the inner radius are approximated as $a_i = R+0.1*R, b_i = R-0.1*R, c_i = R-0.1*R+t_f, b_o = b_i+t_f, c_o = c_i+t_f$.

Let a_o, b_o and c_o be the outer dimensions of the ellipsoid. These are taken as $a_0 = a_i+t_f, b_o = b_i+t_f, c_o = c_i+t_f$. The volume of the half ellipsoid is then approximated as $V_1^{'} = 0.5*\pi*(a_o*b_o*c_o - a_i*b_i*c_i)$. On the front of the ellipse a small cut is given to provide for upward vision. The angle of the cut, as per helmet standards, is 25^0. This cut occupies around 5% of the volume. So the volume of upper part of the helmet reduces to $V_1^{'} = 0.5*0.95*\pi*(a_o*b_o*c_o - a_i*b_i*c_i)$. The height of the elliptical cylinder is taken as 10cm. The volume of the elliptical cylinder is then given by $V_2^{'} = \pi*(a_o*b_o - a_i*b_i)*R$

Part of the elliptical cylinder is open to provide peripheral vision. This part is covered by a glass visor. The angle of opening for peripheral vision is 110^0 with respect to middle vertical plane on its both the sides. The opening occupies approximately 15% of the cylinder space and the face guard occupies around 15%. Then the volume of the foam cylinder reduces by 30%. The total volume thus becomes V_1+V_2 where $V_2 = 0.7*V_2^{'}$. The volume of the foam becomes $V_{foam} = 0.5*0.95*\pi*(a_o*b_o*c_o - a_i*b_i*c_i) + 0.70*\pi*(a_o*b_o - a_i*b_i)*(R)$. The density of the foam depends on density of solid foam and relative density of the foam and is given by d_{foam} = relative density * foam solid density. For the shell a_{si}, b_{si}, c_{si} and a_{so}, b_{so}, c_{so} are the three inner and outer shell dimensions respectively.

Volume of the shell is formulated as
$V_c = 0.5*0.95*pi*(a_{so}*b_{so}*c_{so} - a_{si}*b_{si}*c_{si}) + 0.85*\pi*(a_{so}*b_{so} - a_{si}*b_{si})*(R)$.
Density of composites depends on the density of matrix as well as the density of fiber and is given by $d_c=V_f*d_f+V_m*d_m$. Having estimated the volume and the density of the shell, the mass of the shell can now be estimated.

4. MODEL VALIDATION

After preparing the dynamic model of impact of a crash helmet, the model has been validated against available experimental as well as results from a validated FEM model [3]. Properties of the helmet used for validation are:Inner Foam Layer: Shear Modulus = $9*10^5$ N/m^2, Tangent Modulus = $1*10^5$ N/m^2, Bulk Modulus = $6*10^5$ N/m^2, Yield Stress = $3.2*10^5$ N/m^2, Density = 145 kg/m^3, Thickness of the layer = 25 mm, Outer Shell : Young's Modulus = $1.87*10^9$ N/m^2, Thickness = 37 mm, Stiffness to damping ratio = 0.0133, Velocity of impact = 6.26 m/s. With these values the model is solved to get the acceleration and displacement time history of the helmet. The results obtained are shown in the Fig. 11 which shows the acceleration time history extracted from the discrete dynamic model and FEM analysis. Fig. 12 shows the comparison of the results from the discrete dynamic model with the experimental results.

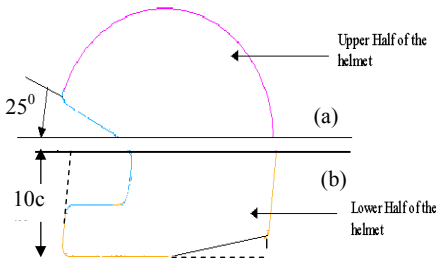

Fig. 10. Geometry of lower and upper half of the helmet.

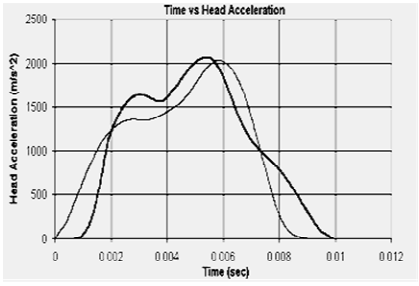

Fig. 11. Acceleration time history of head acceleration.

Peak head acceleration value given by the FEM results is 2030.70 m/s^2, whereas as for the present dynamic model it is 2059.95 m/s^2. The TBPA value given by the FEM model is 1351.05 m/s^2 and the one given by present model is 1542.07 m/s^2. Here we find that the peak acceleration as well as TBPA values given by the present model is higher than that of the FEM model. This shows that the present model is stiffer than the FEM model. In both the models we

observe two prominent peaks and the second peak is higher than the first peak. Fig. 12 compares the experimental results and results of the present model. Two experimental results for the helmet are available. It is evident that TBPA value as well as peak acceleration value is higher in case of theoretical results as compared to practical results. TBPA value for first experimental results is 1362.314 m/s^2 whereas for the second experimental result it is 1491.599 m/s^2. The theoretical peak acceleration value is also higher than the experimental peak acceleration value.
Fig. 13 represents the foam deformation time history for discrete dynamic as well as FEM model. From the figure it can be noted that the maximum deformation given by the discrete dynamic model is lower than the one given by FEM model. The maximum deformation of foam from the dynamic model is 19.67 mm whereas as per the FEM model it is 22.23 mm. Difference between the maximum deformations is 2.56 mm. This again indicates that the discrete dynamic model is giving stiffer results as compared to FEM model. The permanent deformation in discrete dynamic model is 8.678 mm whereas in FEM model is 10.6081 mm.
Thus the developed is slightly stiffer with respect to the experimental results as well as FEM results. The results are however within about 10-12%. This is acceptable in view of the assumptions made for simplification. This model is therefore used for optimization. But before we describe the optimization process, we describe the variation in the behavior of the objective function with respect to the design parameters.

5. SENSITIVITY OF THE DESIGN PARAMETERS

The dynamic model of the helmet impact has been prepared and validated. Having validated the model, we now study the sensitivity of the objective function (TBPA) to the different design parameters.

5.1 Sensitivity wrt Relative Density of Foam

The variation of the TBPA with respect to relative density of foam is represented in the Fig. 14. From the figure it can be observed that the TBPA value increases linearly with increase in foam density. As the relative density of the foam increases, young's modulus of foam increases. This results in increase in stiffness of foam which leads to increase of TBPA value.

5.2 Sensitivity wrt Fiber Volume Fraction

In this case also it can be observed from Fig. 15 that TBPA is linearly proportional to fiber volume fraction. From relation 6.11 it can be observed that Young's modulus of the composite increases with increase in fiber volume fraction. This ultimately leads to increase of stiffness of the shell which results in increase of TBPA value.

5.3 Sensitivity wrt Foam Thickness

From Fig. 16 it is evident that TBPA is high for low values of foam thickness. As the thickness increases the value of TBPA value decreases to a minimum of 1676 m/s^2. Thereafter a slow increase in the TBPA is observed. If the thickness of foam is small, the stopping distance provided by foam reduces drastically and it tends to become solid earlier leading to increase of stiffness. When the foam becomes solid shell stiffness becomes predominant. So with increase in thickness of foam reduction in TBPA is observed.

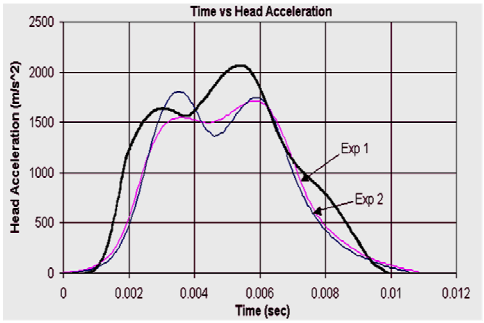

Fig. 12. Acceleration time history of head acceleration (experimental and discrete dynamic model results).

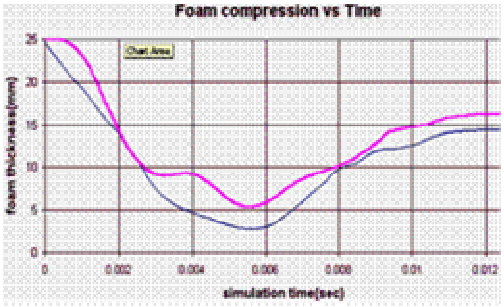

Fig. 13. Foam compression vs time (fem and discrete dynamic model results).

5.4 Shell Thickness

In case of shell thickness, as shown in the Fig. 17, it is found that the TBPA value increases for the initial range of 3 mm to 4.2 mm. After that the value starts dropping down. Thus a minima will be obtained in both the ranges. But the

one found in lower range will be important from view point of mass constraint. Fig. 18 is a surface graph presenting the variation of objective function i.e. TBPA with respect to variables related to foam i.e. relative density of foam and its thickness. From the figure it is clear that the objective function is higher for low thickness and for high relative density, whereas it is lower for low relative density and higher foam thickness. In this region of low relative density and higher foam thickness, it can be observed that the surface is quite flat and the variation in the objective function value is less. Fig. 19 is another surface plot representing the objective function variation with respect to variables related to shell i.e. shell thickness and fiber volume fraction. It can be observed that the objective function value is lower in two regions; One corresponds to high fiber volume fraction and higher thickness and another one corresponds to low fiber volume fraction and lower thickness.

6. OPTIMIZATION

In optimization we aim to find optimal values of material properties and geometric parameters like thickness of different parts of the helmet. The different aspects of the problem are as follows:

The prime focus of the optimization is to maximize the protection provided by the helmets. This protective efficiency is measured using head injury criteria. In this work the TBPA is chosen as the criterion for optimization. This optimization has been subjected to a set of constraints. The neck takes up the weight of the helmet. So use of heavy helmet may lead to neck injury in long term use. Thus to satisfy the ergonomic considerations, the weight of the helmet should not exceed 1.3 kg [15]. As total mass of the helmet is non-linear function of material properties and geometry of the helmet, this is nonlinear type of inequality constraint. Another constraint is put on the total thickness of the helmet. It is maintained below 35mm [15]. This is linear type of inequality constraint.

The optimization problem can now formally be stated as follows:

Design Parameters: Relative density of foam (D), Fiber volume fraction (V_f), Inner Foam layer thickness (t_f)
Outer shell thickness (t_s)

Objective function: Minimize TBPA

Constraints: Non-linear : $m_s + m_f \leq 1.3$, Linear constraint : $t_s + t_f \leq 35$

In the present work two different approaches have been adopted for optimization, viz, a sequential quadratic programming approach and Genetic Algorithms (GAs).

7. RESULTS AND DISCUSSION

The results obtained from the 'sequential quadratic programming' approach are presented in Table 1. Different initial values were given in different runs to ensure that the algorithm did not get stuck with a local optima.

The same problem was solved by the genetic algorithms also. For different initial values genetic algorithm gave same result. The results are presented in the Table 2. It can be observed that the optimal values match with the lowest minima obtained by the conventional method. It was also observed that the results from GAs were more consistent.

The graphical results for the optimized parameters are presented in Fig. 20 to Fig. 23. The peak value of the acceleration is 2237.1m/s^2 where as the TBPA is 1676.1 m/s^2 . the maximum deformation of the inner foam layer is 16.7mm. The permanent deformation of foam observed is 13.89 mm. For shell the maximum deformation goes is 0.129 mm. It remains in elastic region throughout the deformation. So it regains its original shape. The maximum movement of the head in the downward direction is 20.13mm. In order to understand the functioning of the helmet, let us look at the foam and shell deformations closely. From Fig. 23 we can observe six prominent stages of the time history plots according to the motion of the head form and helmet. These stages are marked with points A, B, C, D, E and F in the figure. The movements of the head and the helmet in these stages are presented diagrammatically in Fig. 24.

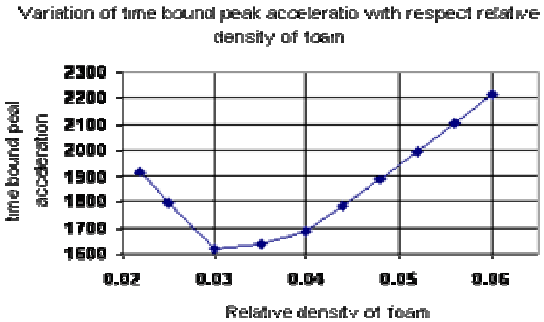

Fig. 14. Variation in TBPA with respect to relative foam density.

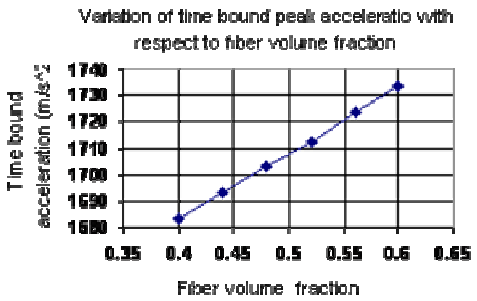

Fig. 15. Variation of TBPA with respect to fiber volume fraction.

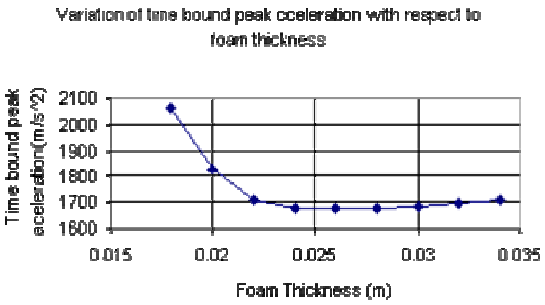

Fig. 16. Variation of TBPA with respect to foam thickness.

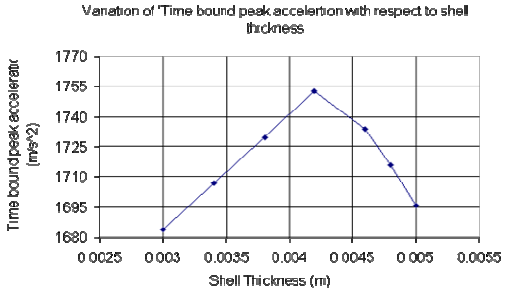

Fig. 17. Variation of TBPA with respect to shell thickness.

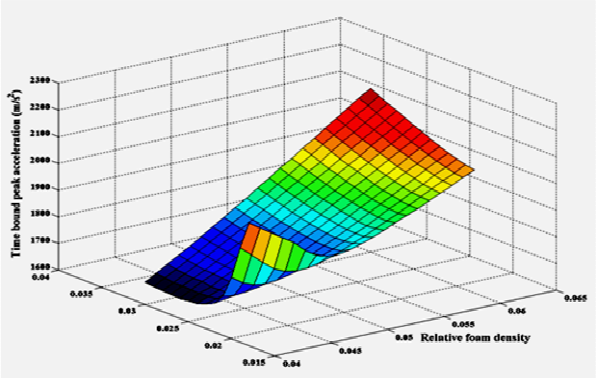

Fig. 18. TBPA vs foam relative density and foam thickness.

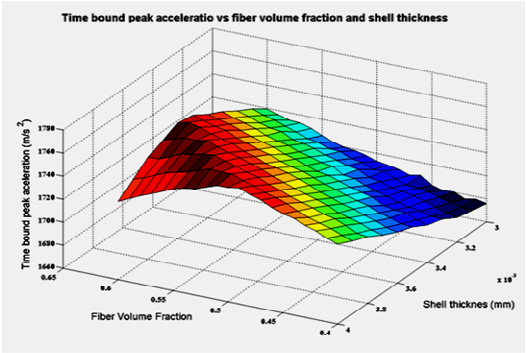

Fig. 19. TBPA vs shell thickness and fiber volume fraction.

	INITIAL GUESS D, V_f, t_f (mm), t_s (mm)	**FINAL SOLUTION** D, V_f, t_f (mm), t_s (mm)	**VALUE OF OBJECTIVE FUNCTION**
1	0.04, 0.4, 18, 2.9	0.04, 0.4, 26.2, 3	1676.5
2	NO	0.04, 0.5204, 22, 3.2	1715.1
3	0.04, 0.6, 28, 3	0.04, 0.4, 0.04, 0.004	1683.7

Table 1. Result obtained by using conventional method.

NO	**FINAL SOLUTION** D, V_f, t_f (mm), t_s (mm)	**VALUE OF OBJECTIVE FUNCTION**
1	0.0402, 0.4067, 26.4, 3.07	1681.1

Table 2. Results obtained by using genetic algorithms.

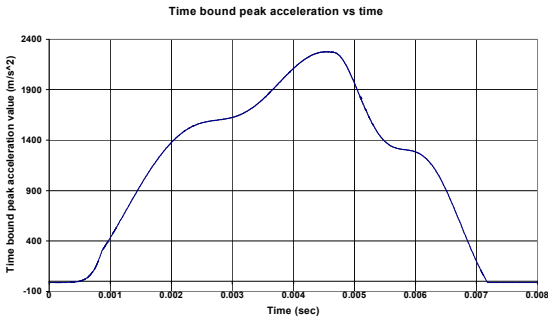

Fig. 20. Acceleration vs time for optical solutions.

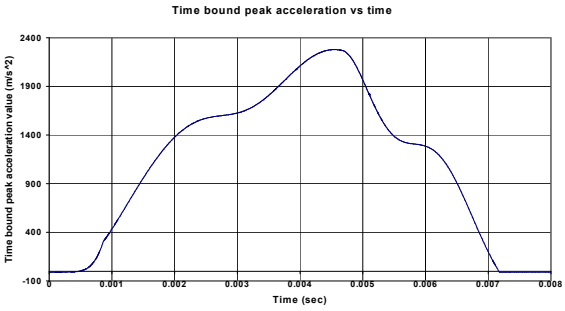

Fig. 21. Shell deformation vs time for optimal solution.

The stages and their relation with acceleration is explained as follows:
First Stage: (0 – 0.0009 sec): In the first stage both helmet and headform move towards the impact plane. The helmet hits the impact plane and its velocity decreases to zero while the velocity of the headform is constant.

Second Stage: (0.0009 – 0.0022 sec): In the second stage headform is still moving downwards. But the helmet (foam layer and shell) moves upward pressing the headform hard. This increases the head acceleration faster as can be seen from acceleration time history plot in Fig. 20.
Third Stage: (0.0022 – 0.0034 sec): In the third stage helmet again starts moving downwards due to the momentum of the head. This increases the foam compression and the compressive forces between headform and the foam. This leads to slight reduction in the headform acceleration.
Fourth Stage: (0.0034 – 0.0047 sec): In the fourth stage the headform continues to move downwards and the helmet bounces back and moves upwards. This again causes hard pressing of the foam layer. This increases the compressive forces at the contact between headform and the foam and increases the headform acceleration.
Fifth Stage: (0.0047 – 0.0054 sec): Thereafter in the fifth stage, head moves down whereas the headform starts moving up. Due to these movements, the compression in the foam layer is released causing reduction in the forces. This reduces the headform acceleration.
Sixth Stage: (0.0054 sec onwards): In this last stage the headform continues to move up as well as the helmet bounces back and starts moving up. The helmet pushes the headform causing small increase in the foam compression. This reduces the acceleration for a while as seen from the Fig. 20.

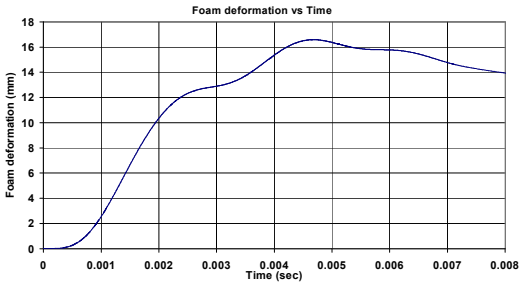

Fig. 22. Foam deformation vs time history for optimal solution.

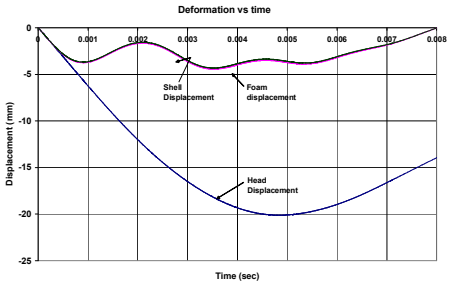

Fig. 23. Head, foam and shell deformations vs time.

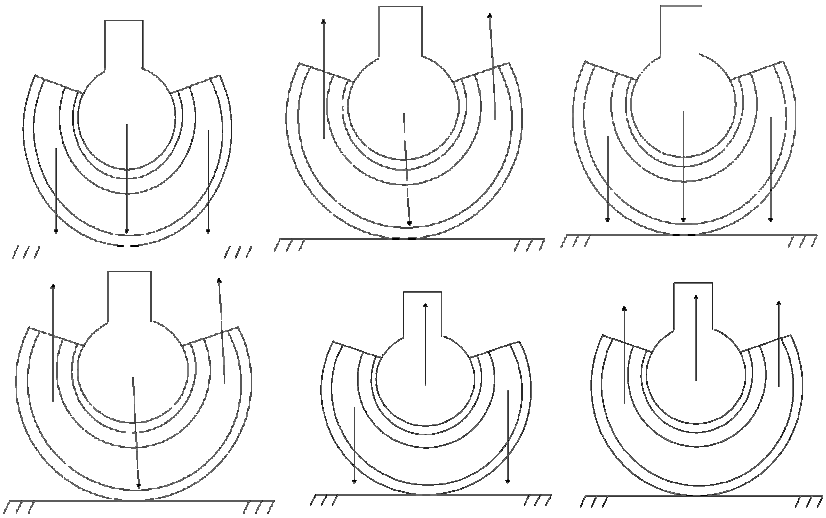
Fig. 24. Six Stages Of Helmet Impact.

8. REFERENCES

[1] Brands, D. W. A., Thunnissen, J. G. M. and Wismans, J. S. H. M., Modeling Head Injury countermeasures a: 3D Helmet model, AGARD Specialists' meeting on impact head injury: responses, mechanisms, tolerance, treatment and countermeasures, 1996, pp 261- 267.
[2] Chaner, S., Gilkhrist, A. and Mills, N. J., 1991, Motorcycle Helmet Load spreading performance of impact into rigid and deformable objects, Proceedings of IRCOBI, Conference on Biomechanics of impact, 1991, pp 24

[3] Daniel, I. M. and Ori Ishai, Engineering Mechanics of Composite Materials, Oxford University Press(First Edition), 1994.
[4] Iain, F. and Heller, W. R., Creep of engineering Materials, MacGraw-Hill Book company, First Edition, 1959.
[5] Gilchrist, A., Mills, N. J. and Rowland, F.J., 1988, Mathematical Modeling of the Effectiveness of Helmets in head protection, Proceedings of IRCOBI, Conference on Biomechanics of impact, 1988, pp 215-226.
[6] Gilchrist, A. and Mills, N. J., 1994, Protection of the side of the helmet, Proceedings of IRCOBI, Conference on Biomechanics of impact, 1994, pp 81-94.
[7] Goldsmith, W., Meaningful Concepts of Head Injury Criteria, Proceedings of IRCOBI, Conference on Biomechanics of impact, 1989, pp 1-11.
[8] Kraus, H., *Thin Elastic Shells*, John Wiley & Sons, Inc., 1967.
[9] Hilyard, N. C., Cunningham A., *Low Density Cellular Plastics Physical Basis of Behavior*, Chapman and Hall, (First Edition).
[10] Hopes, P. D. and Chinn, B. P., Helmets: A New Look at Design and Possible protection, Proceedings of IRCOBI, Conference on Biomechanics of impact, 1989, pp 39-53.
[11] Mills, N. J., Accident investigation of motorcycle helmets, *Journal of the Institute of Traffic Accident Investigators*, Volume 5, 1996, pp 46-51.
[12] Mukherjee, S, et al, Motor Cycle – Wall Crash: Simulation and Validation, Proceedings of the Pam Users Conference Asia, 2001.
[13] Otte, D., Jessl, P. and Suren, E. G., Impact Points and Resultant Injuries to the Head of Motor–Cyclist Involved in Accidents, with and without Crash Helmets, Proceedings of IRCOBI, Conference on Biomechanics of impact, 1984, pp 47-64.
[14] Pipkin, P. C., *Lectures on Viscoelasticity Theory*, George Allen & Unwin Ltd.,1972.
[15] Rao, K. L., Dynamics of Helmet structure, M.Tech thesis, Mechanical Engineering Department, IIT Delhi, 1998.
[16] Stocker, U. and Lofferholz, H., Investigation into the Protective Effects of Helmets on Users of Powered Two-Wheelers, Proceedings of IRCOBI, Conference on Biomechanics of impact, 1984, pp 79-90.
[17] Vallee, H., Hartemann, F., Thomas, C. and Tarriere, C., The Fracturing of Helmets, Proceedings of IRCOBI, Conference on Biomechanics of impact, 1984, pp 99-100.
[18] Willinger, R, Guimber, T, McLean, A. J., Anderson, R. and Farmer, M., Experimental and theoretical modeling of head impact, Proceedings of IRCOBI, Conference on Biomechanics of impact, 1996, pp 21-34.